applied sciences

MDPI

Article

Application of Bender Elements Technique in Testing of Anthropogenic Soil—Recycled Concrete Aggregate and Its Mixture with Rubber Chips

Katarzyna Gabryś [1,*], Wojciech Sas [1], Emil Soból [2] and Andrzej Głuchowski [1]

[1] Water Centre-Laboratory, Faculty of Civil and Environmental Engineering, Warsaw University of Life Sciences, 02-787 Warsaw, Poland; wojciech_sas@sggw.pl (W.S.); andrzej_gluchowski@sggw.pl (A.G.)
[2] Department of Geotechnical Engineering, Faculty of Civil and Environmental Engineering, Warsaw University of Life Sciences, 02-787 Warsaw, Poland; emil_sobol@sggw.pl
* Correspondence: katarzyna_gabrys@sggw.pl; Tel.: +48-22-593-5405

Academic Editor: Jorge de Brito
Received: 30 May 2017; Accepted: 17 July 2017; Published: 21 July 2017

Featured Application: Recycled Concrete Aggregate can be a very good alternative material for natural aggregate. Using soil-rubber mixture as an engineering material may not only provide alternative means of reusing waste but also significantly change dynamic properties of soil.

Abstract: This paper discusses the application of piezoceramic bender elements (BEs) for measurement of shear wave velocity in the time and frequency domain in a triaxial cell under different isotropic confinement. Different interpretation methods were used in the tests and their results were finally compared with each other. Two types of anthropogenic material were tested: pure Recycled Concrete Aggregate (RCA) and RCA-rubber chips mixtures (15% of rubber addition). Presented study is an attempt to describe dynamic properties, in terms of shear wave velocity (V_S), of the aforementioned anthropogenic material using the technique commonly applied for natural soil. Although some research is currently being carried out, in order to evaluate physical, chemical and mechanical properties of RCA and rubber-soil mixtures, still little is known of their dynamic properties. Hence, this work will provide the experimental results of shear wave velocity of RCA and its modified version. The results show that tires chips significantly decrease the V_S values of modified RCA. They help to reduce the near field effect, but the received parameters are more incoherent. The V_S values were found to be influenced by interpretation technique, mean effective stress and wave's propagation period. The maximum V_S values were obtained mostly from the frequency domain method, although time domain analysis gives the results that are more coherent.

Keywords: anthropogenic soil dynamics; bender elements tests; shear wave velocity; recycled concrete aggregate; rubber chips

1. Introduction

The realization of the importance of soil stiffness, represented generally by shear modulus (G), at low shear strain level ($\gamma < 10^{-5}$), in both static and dynamic behavior, has led to increased interest in methods of measuring stiffness at small strains in the laboratory. One of the most used technique to establish shear wave velocity (V_S), and therefore shear modulus [1], is to make use of bender elements (BEs), small piezoceramic devices that can generate and detect waves in soil [2].

V_S is an important parameter for the design of geotechnical systems [3], particularly in seismically active areas [4,5]. It is necessary for design and site response purposes, is related to stiffness of a foundation, evaluation of site response during earthquakes, liquefaction potential [6], site

characterization, soil density and its stratigraphy, or settlements of foundations [7]. On the other hand, the anthropogenic impacts, like mining tremors, use of roads and rails transport etc., cannot be ignored as well. Some high-speed transport systems (e.g., expressway, high-speed railway, and airstrip) have been recently developed a lot, which transmit dynamic loading to subsoil. The settlements of subsoil in these cases are very much related to soil stiffness. Information of shear wave velocity is crucial for a better knowledge of work capacity of soil.

Shear wave velocity is connected to the small-strain shear modulus (G_{max}) using elasticity theory:

$$G_{max} = \rho \cdot {V_S}^2, \quad (1)$$

where ρ means mass density of the material (equal to the total unit weight of the material, γ_t, divided by the gravitational acceleration) [8]. It is also recognized that shear wave propagation is the most versatile and portable method to assess G_{max} in the laboratory, besides bender elements [9], resonant column tests [10], and in the field, e.g., cross cone, seismic cone and surface waves methods [11].

The desire to improve of the road infrastructure in Poland has led engineers to construct, inter alia pavements in various conditions. A request of construction materials in such a situation enhances a great need to explore new ways of reuse of waste deposits. Economic development in Poland has recently induced many deposits of Construction and Demolition (C&D) materials, such as demolished brick and concrete. On the other hand, an increase of ecological awareness has also caused bigger concentration on recycle building wastes and their possible usage in engineering constructions. In the field of pavement engineering, C&D recycling materials, like other composite materials [12], have been used in roads, embankments, pipes bedding and backfilling [13]. This trend has become global standard of treating crushed concrete and other construction materials [14,15].

The subject of this research is Recycled Concrete Aggregate (RCA), an example of anthropogenic material, which is a product of demolishing of exploit constructions [16]. The authors investigate the behavior of plain RCA as well as its mixture with rubber grains. One of the waste types produced during cars' exploitation and after their utilization are rubber tires [17]. Disposal of waste tires has become a global problem [18]. Effectively reusing waste tires is an urgent and important issue for saving energy and protecting the environment [19]. Scrap tires, shredded into small pieces (called "chips"), alone or mixed with soil can have properties favorable to civil and environmental engineering applications [20]. Recycled waste tires when mixed with soil can play an important role as lightweight construction materials in embankments, retaining walls, machine foundations and railroad track beds in seismic zones. Rubber can be presented as an alternative material in various construction activities, because it is cheap and available in abundance. It can reduce vibrations when seismic loads are of great concern or even improve some mechanical properties of problematic soils, e.g., soft soils [21].

Over the last decades, there have been many investigations, which highlighted physical, chemical and mechanical properties of RCA. Numerous researchers have conducted studies to determine the same parameters but of rubber-soil mixtures [22]. To authors' knowledge, data on shear wave velocity of concrete aggregates with rubber chips is, however, remarkably limited. Therefore, the scientific objective of this work is to recognize and evaluate the V_S values of such anthropogenic material from modern geotechnical research technique originally applied for natural soil, i.e., bender elements set in the triaxial device, in the time and frequency domain.

2. State of the Art

Most of the work presented in the literature concerns mechanical properties of RCA [23], durability and/or volume stability. Direct Shear Tests (DSTs), conducted by Soból et al. [24] and Arulrajah et al. [25], showed that among six tested C&D materials all meet the shear strength requirements for aggregates in pavement engineering, including RCA. Melbouci [26] in 2009 carried out cyclic loading tests on RCA samples with addition of sand and concrete. Laboratory research, typical for roads, were also performed on a large scale, including California Bearing Ratio (CBR) [27],

compaction, crushing susceptibility, freeze thaw and triaxial tests [28] or long-term cyclic triaxial tests [29]. Nonetheless, studies on dynamic properties (shear modulus and damping ratio) of RCA are still very few [30].

In the recent past, a series of intensive studies, aimed at finding the possible application of rubber chips mixed with natural aggregates, have been conducted as well. Takano et al. [19] tested shear behavior of rubber chips and silica sand mixture using micro focus X-ray CT scanner. The results of those tests proved that, while direct shearing of the mixture of sand and rubber chips, the shear stress level rises monotonically and no peak stress is observed. Dilatancy effect was also not very significant, in comparison to the tests conducted on pure sand. It was also interesting that rubber chips additions can decrease shear strain propagation. This fact turned to be important for road engineering, as shear stress causes many structural damages. For instance, Srinivas et al. [31] studied a mixture of gravel, fly ash and waste fibers. Their study revealed an increase of CBR characteristics, namely optimal addition of waste tire rubber ranged between 0.2% and 2.0% of dry unit weight of soil. Two scientists, Ghatge and Rakaraddi [32] in 2014, though, used shredded waste rubber for reinforcement of soft clay with different percentages of rubber content and, additionally, with cement as a binding medium. CBR test set, together with unconfined compressive strength tests, pointed out an improvement of bearing capacity, strength and high compressibility of the tested material.

However, only a limited number of research described the cyclic behavior, including the liquefaction potential and dynamic properties of sand-scrap tire mixtures (e.g., [33–35]). Turer and Özden [36] reported that sand-scrap tire mixtures have lower shear modulus and higher damping ratio compared to sand at low to medium shear strains ($\gamma < 0.1\%$), while pure scrap tires have higher damping ratio. Kaneko et al. [37] stated that sand-tire crumb mixtures show remarkable damping and seismic isolation properties. They have an ability to reduce significantly the acceleration amplitude at the ground surface, due to the low stiffness of tire crumbs. Because of the lack of experimental data, Tsang et al. [38] studied dynamic properties of scrap tire-soil mixture based on the extrapolated data of shear modulus and damping ratio of Feng and Sutter [33] for shear strains greater than 0.1%. Mashiri et al. [34] conducted a series of strain controlled consolidated undrained cyclic triaxial tests on specimens of sand mixed with varying proportions of tire chips. The maximum shear modulus (G_{max}) of the tested mixture was determined by bender element tests for different gravimetric proportions of tire chips and various effective confining pressures. The initial shear modulus was found to be influenced by the proportion of tire chips and confining pressure. The results showed as well that the increase of scrap tire in sand-scrap tire mixtures reduced shear modulus degradation curves and increased damping ratio curves. Anbazhagan and Manohar [22] in 2015 investigated static properties (i.e. shear strength and energy absorption capacity) of Sand Tire Crumb Mixtures (STCM), and then in 2016 [39] they presented dynamic properties of STCM in terms of G and D against shear strain (γ). Torsional resonant column tests were performed to measure G and D of the small strain rate of 0.0001% to 0.1%. Their values at a large strain rate (0.1% to 10%) were measured through cyclic triaxial test. The results showed that shear modulus and damping ratio of the mixtures were strongly influenced by the percentage of rubber inclusion. Shear modulus decreased with an increase in tire crumb inclusion for all confining pressures, whereas damping ratio increased with the increase in rubber content in STCM. For any percentage of tire crumbs inclusion, shear modulus increased and damping ratio decreased with increasing confining pressure. Ehsani et al. [21] also conducted torsional resonant column and dynamic triaxial experiments of sand-granulated rubber mixtures. They examined the effect of rubber content and ratio of mean grain size of rubber solids versus soil solids ($D_{50,r}/D_{50,s}$) on dynamic response of these mixtures, in a range of low to high shearing strain amplitude, from about 4×10^{-4}% to 2.7%. Similar conclusions, as in the case of previously cited studies, were drawn. It is worth emphasizing that a decrease in $D_{50,r}/D_{50,s}$ caused the mixture to exhibit more rubber-like behavior.

Regardless of immense work performed by various researchers to determine physical, chemical, mechanical and, sometimes as well, dynamic properties of RCA and rubber-soil mixtures, the authors were unable to find the detailed study of V_S of RCA improved with rubber grains, covering the wide range of strains, from small to moderate strains (0.0001% to 0.1%). Therefore, such a complete study on RCA with rubber chips will help to fill this gap in the geotechnical engineering knowledge, provide new information about this modified anthropogenic soil and may be very useful for selecting the shear modulus and damping values associated with field events, e.g., machine foundations, motion characteristics or earthquake motion.

Nowadays in Poland, in the field of transportation and/or road investments, anthropogenic soils can be easily located. The decision either to leave them, or to exchange for a better material, must result from studies of their behavior. In addition, the rapid development of modern civil engineering constructions as well as EU directives force engineers to use anthropogenic soil nevertheless. It must be supported by the extensive knowledge of their engineering properties, including dynamic ones.

3. Experimental Program

3.1. Materials Used

In this study, demolished concrete from building demolition site and industry produced scrap tires from Warsaw, Poland were used. Concrete aggregates were an element of concrete floors, especially concrete curbs from demolition of roads. The age of this material is about 20 years. For the purpose of this research, the authors purchased the aggregates of concrete from the crusher company. The strength class of concrete from which the aggregates were formed was estimated between C16/20 and C30/35. In 99% of weight, the aggregates were composed of broken cement concrete and in 1% of glass and brick (Σ (Rb, Rg, X) $\leq$ 1% m/m), in accordance with Polish Committee for Standardization [40]. They did not contain asphalt or any tar elements. The basic properties of original concrete are shown in Table 1. Grain gradation curve was adopted in respect to WT-4 [41] and placed between upper and lower grain gradation limits. These limits are typical for the upper layer of the improved substrate [41]. Concrete aggregates required preliminary research on saturation in order to prevent the movement of water necessary for hydration [42]. The material did not show any binding properties. Recycled Concrete Aggregates needed for the specimens are shown in Figure 1.

Table 1. Basic physical properties of original concrete.

Description	Unit	Value
Apparent density	kg/m^3	1900–2500
Porosity	%	12–15
Impregnability	%	2–8
Water absorption	%	4–14
Mineral dust content	%	7
Contamination content	%	2–12
Sulfur compounds content	%	0.2–0.6
Crushing index	%	2.5–5.5

(**a**) (**b**)

Figure 1. Coarse aggregates for RCA with a size less than 8.0 mm. (**a**) Coarse aggregates; (**b**) particle size.

Granular rubber in the presented research was shredded and processed in the local tires manufacturing plant. Only one size of rubber, without steel belts, was bought and then applied in the experimental program. It was fine granular rubber (i.e., rubber chips) with the maximum particle size less than 1.0 mm. Generally, the employed rubber grains were with the diameter size between 0.06 and 0.4 mm (Figure 2).

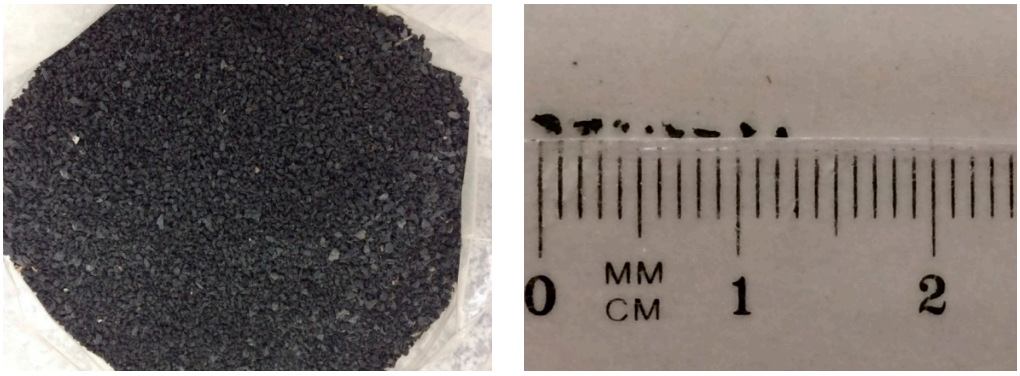

(**a**) (**b**)

Figure 2. Rubber chips used in this study with a size of 0.06–0.4 mm. (**a**) Rubber chips; (**b**) particle size.

3.2. Specimens Preparation

In order to evaluate physical properties of examined material, a set of tests was conducted. As the first one, the grain size analysis (sieve analysis) was performed. The particle size distribution of Recycled Concrete Aggregate used in this study is presented in Figure 3. This analysis led to classification of the tested material as gravel with sand (*saGr*), according to European Committee for Standardization [43]. The values of the characteristic diameters (d_{10}, d_{30}, d_{50}, d_{60}) and coefficients (C_u, C_c), typical characteristics for natural soils by Polish Committee for Standardization [44], are attached to Figure 3 as well. For instance, d_{50} is an average diameter, or otherwise measurable. It is along with larger grains 50% of specimen's weight. Here, it was d_{50} = 2.60 mm and could be used to determine the shape of grain size distribution. The specimen's coefficient of uniformity (C_u) and coefficient of curvature (C_c), corresponding to $C_u = \frac{d_{60}}{d_{10}}$ and $C_c = \frac{{d_{30}}^2}{d_{10} \cdot d_{60}}$, amounted C_u = 9.09 and C_c = 2.92, respectively. C_u is a crude shape parameter, which allows classifying soil gradation, whereas C_c is a coefficient to characterize gradation indicating, e.g., the potential of interlocking. The values of these coefficients suggest a well-graded material, susceptible to compaction process and suitable for the construction of embankments. This distribution of particles from 8.0 to 0.063 mm is typical for soils designed for improved sub-base and supporting other structures.

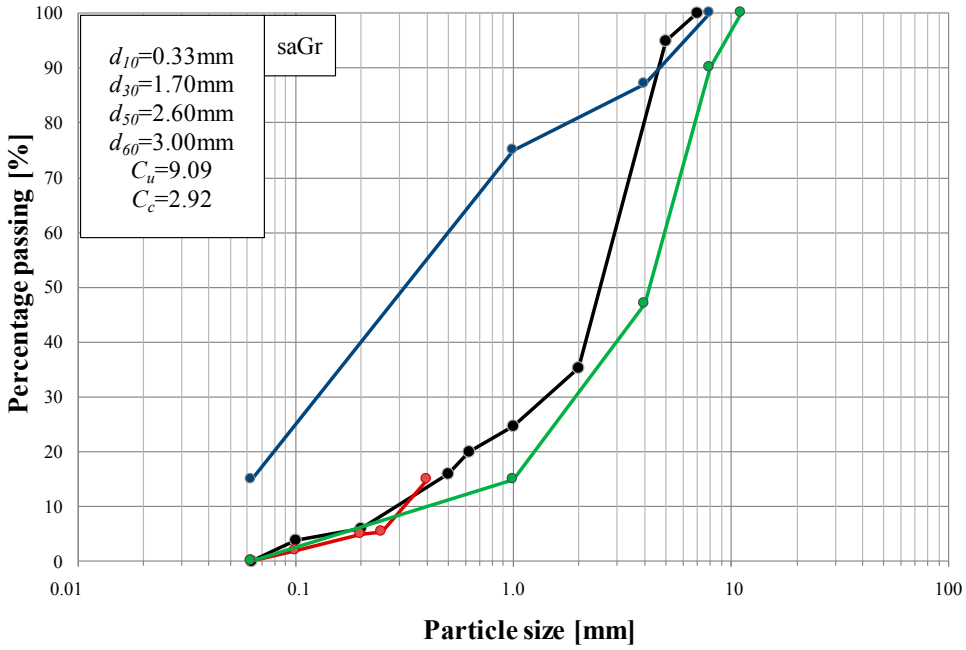

Figure 3. Particle size distribution of RCA and rubber chips (black line: pure RCA, red line: rubber chips, blue line: upper limit by WT-4 [41], green line: lower limit by WT-4 [41]).

As the next study, the standard compaction tests were carried out in order to determine the optimum moisture content (w_{opt}) and the maximum dry density ($\rho_{d\max}$) of RCA. The following results were obtained: w_{opt} = 10% and $\rho_{d\max}$ = 1.96 g/cm^3.

Then, the exact amount of RCA and rubber chips was estimated, in order to prepare an appropriate composition of ingredients. The mixture was prepared by hand mixing of rubber chips with RCA. The authors decide to use the same gravimetric proportion of rubber chips for all three specimens, namely 15%. The new material is shown in Figure 4. The finest fraction of RCA was removed and replaced by grains (Figure 3). The reason for eliminating only the finer fraction of RCA and tempering it by particles from tires was to obtain a material with better values of coefficients C_u and C_c so that it would be non-uniform and well graded. Furthermore, the undesirable feature of fine fractions is the possibility of re-binding which the authors indented to avoid. The introduction of rubber into anthropogenic soil was aimed as well to prevent from eventual negative effects of water filtration.

Figure 4. Prepared composition of RCA with rubber chips.

Subsequently, the modified recycle concrete aggregates were transferred into the special mold with layers with uniform mix to avoid segregation during the specimens' preparation. In this study, the tamping method was adopted to prepare specimens with the correct dimensions, i.e., 70 mm of diameter and 130 mm of height. All specimens were prepared in the same manner in order to guarantee the same compaction energy applied to the samples. All specimens were characterized by the same moisture conditions, equal to optimum moisture content, as mentioned earlier. The compaction procedure was the same as defined by Proctor test [30]. The selected method is characterized by the use of a 2.5 kg hammer with diameter of 3.0 cm, lowered from a height of 10.0 cm to a large mold with volume of 2.2 dm^3. A 5-layers Proctor test was performed, with 24 blows to each layer. This procedure creates constant energy of compaction; whose level is equal to 0.59 J/cm^3. The initial properties of three pure RCA specimens and three RCA-rubber chips compositions are presented in Table 2. Six tested specimens differed from each other with the mean effective stress value (p') applied during consolidation stage. After the preparation process was finished, the bender elements tests were carried out.

Table 2. Initial properties of pure RCA specimens and mixtures of RCA with rubber chips.

Description	Unit	Pure RCA			RCA with Rubber Chips		
		No. 1	No. 2	No. 3	No. 4	No. 5	No. 6
		Value					
Initial water content	%	6.93	14.91	6.67	9.59	8.54	9.64
Bulk density of soil mass	g/cm^3	1.75	1.88	1.79	1.32	1.36	1.32
Soil particle density	g/cm^3	2.60					
Bulk density of soil skeleton	g/cm^3	1.64	1.63	1.68	1.20	1.25	1.20
Void ratio	-	0.59	0.59	0.55	1.16	1.08	1.17
Saturation ratio	%	0.31	0.66	0.32	0.21	0.21	0.21

3.3. Methodology

Bender elements have been widely utilized to measure V_S at low strain levels, namely $\gamma < 0.001$ percentage [45]. The simple operation of these piezoceramic transducers, together with their small size, has stimulated their use in a big variety of geotechnical equipment since their first appearance [46]. BEs have been incorporated into a wide range of laboratory device (i.e., triaxial [47], true triaxial, hollow cylinder, simple shear, shear box, oedometer, resonant column), as well as into boundaries of laboratory model test apparatuses. Originally, BEs were applied to determine G_{max}, but with the passage of time and their greater usage, they have been employed to measure P-wave velocity (V_P), to investigate fabric and structure, additionally in particular cementation and its degradation, degree of saturation or anisotropy, to assess sample's quality and control multi-stage testing [48].

However, BE testing is not yet a standard, due to the variability of its results in comparison with standard resonant column testing [45]. The reliability of BE technique is influenced by different factors, e.g., near-field effects [49], directivity [48], travel distance [50], boundary effects [51], sample geometry and size [52], cross-talking [53]. The difficulty lies as well in accurately evaluating the travel time (tt) of shear wave from the source BE to the receiver BE, whereas a distance between elements (L_{TT}), accepted as the tip-to-tip distance, can be precisely measured. V_S is then calculated in accordance with the formula:

$$V_S = \frac{L_{TT}}{tt}. \quad (2)$$

The operating principles of a BEs system have been described in many previous studies of the authors, e.g., [54].

The time domain and frequency domain analysis were applied in this work to estimate the travel time. The time domain methods are the mostly widely used. These techniques are referred to an

analysis made from signals represented along the axis of time in which the input and/or output waveforms are plotted. Two points of these graphs can be selected following a given criterion, where their time difference is defined as the travel time between the transmitter and receiver of the analyzed wave [55]. A typical output signal gathered from a step input signal is presented in Figure 5. Estimation of *tt* by the identification of the first direct arrival in the output signal was the initial assumption in this method. This assumption is an intuitive interpretation following the method used on in situ geophysical measurements and was the interpretation method initially adopted [46]. The method remained unchanged for nearly 10 years until a travel-time determination based on the first inversion of the received signal was proposed [56]. What is, however, the appropriate first arrival point: A, B, C or D? Suggested criteria and recommendations are various and differ depending on installation, application, and input signal [53]. First arrival detection methods can be affected as well by near field effects with low-frequency input waves [51,53], which result from BEs generating lateral P-waves reflection and refraction from specimen boundaries, and by signal noise at higher frequencies.

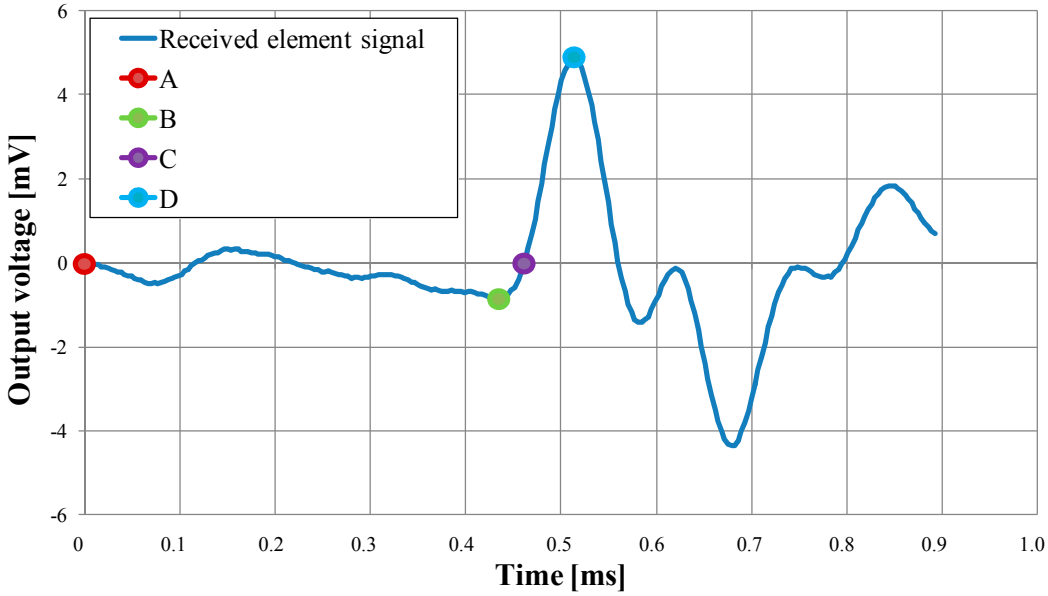

Figure 5. Receiver time charts: A) first deflection; B) first bump; C) zero crossing; D) first major peak. An example of test results from pure RCA specimen No. 2, T = 0.16 ms, p' = 90 kPa.

Several researchers, like Greening and Nash [57] have proposed the frequency domain methods, because they potentially allow automation of signal processing and avoid the difficulties associated with picking the first arrival. On the other hand, these techniques are either unreliable or require considerable user intervention to provide a reasonable result. A unique criterion for the travel time determination is here elusive [48]. Cross-correlation is considered to be one of the time domain methods, although all calculations are performed in the frequency domain. Cross-correlation essentially measures the level of correspondence between the transmitted and received signals: transmitted, *T(t)* and received, *R(t)*, as expressed by the cross-correlation coefficient, CCTR (t_s):

$$CC_{TR}(t_S) = \lim_{T_r \to \infty} \frac{1}{T_r} \int_{T_r} T(t + t_S) R(t) dt, \quad (3)$$

where T_r is the time record and t_S is the time shift between the two signals.

Using the same signals as for previously mentioned techniques, the cross-correlation function is plotted alongside the transmitted and received signals (see Figure 6). The cross-correlation values are calculated from the source and received element signals at each time stamp of the data. The time at

which the maximum cross-correlation value occurs is then used to estimate the travel time of shear wave [58]. In order to apply this technique, it is convenient to convert the time domain signals to the frequency domain, whereby decomposition of the signals produces groups of harmonic waves with known amplitude and frequency. A common algorithm used for this purpose is the Fast Fourier Transform (FFT), which transforms the signals to their linear spectrums, giving the magnitude and phase shift of each harmonic component in the signal, respectively. The complex conjugate of the linear spectrum of the transmitted signal is next computed, and the cross-power spectrum of the two signals established [59].

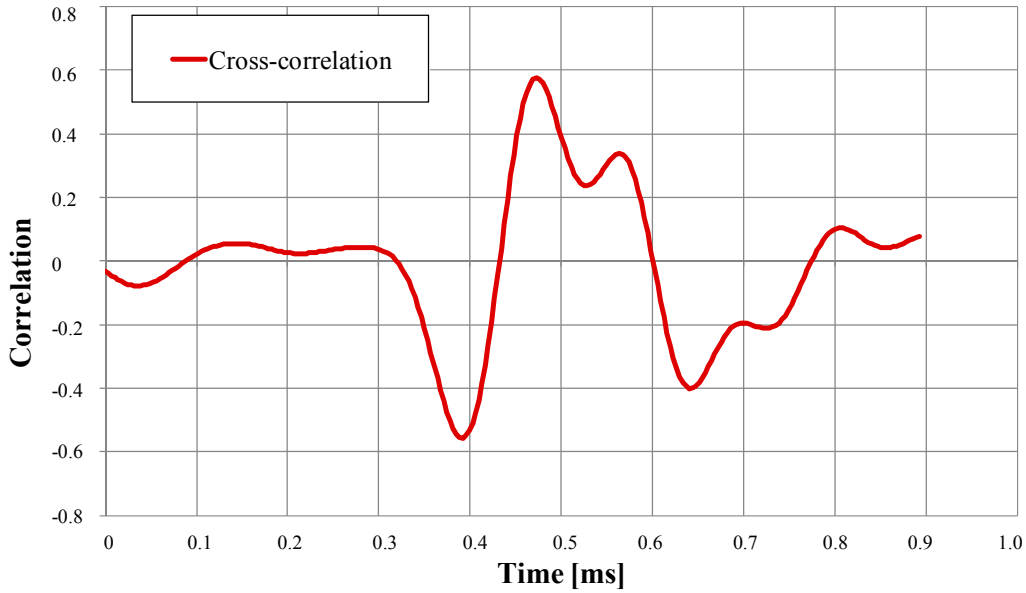

Figure 6. Cross-correlation method. An example of test results from pure RCA specimen No. 2, T = 0.16 ms, p' = 90 kPa.

Viggiani and Atkinson [56] also first proposed implementation of the cross-spectrum method in analyzing results from the bender element test. It is essentially to have an extension of the procedure used in the cross-correlation method, where the frequency spectra of the signals are further manipulated to obtain the absolute cross-power spectrum. The cross-power spectrums, obtained via FFT, are used to create a phase angle versus frequency plot. The slope of this plot is then used to estimate the shear wave travel time, based on a linear best fit across a defined frequency window [58]. An example of the unwrapped phase is displayed in Figure 7. The frequency domain calculations are related in this paper to the cross-spectrum analysis.

3.4. Testing Procedure

The Consolidated Drained triaxial tests were carried out on six specimens, with the same dimensions, in Water Centre-Laboratory, Warsaw University of Life Sciences, Poland. When specimens were completely prepared, standard initial steps of triaxial tests were performed, i.e., flushing, saturation and consolidation. The first three specimens, of pure RCA, were consolidated under different mean effective stress (p'), by the following scheme: p' for specimen No. 1 was equal to 45, for No. 290 and for No. 3180 kPa. Then, the same testing program was applied to three mixtures of RCA with rubber chips. After the consolidation stage finished, BEs tests started.

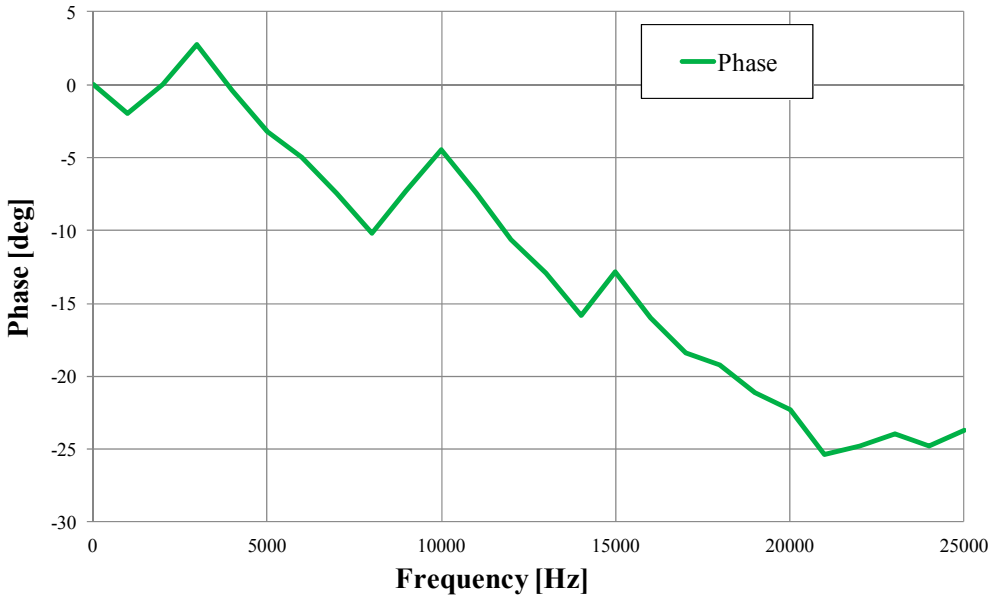

Figure 7. "Unwrapped" phase in cross-spectrum method. An example of test results from pure RCA specimen No. 2, T = 0.16 ms, p' = 90 kPa.

BEs were installed in the triaxial apparatus, in a top cap and pedestal (Figure 8). Those BEs are made from piezoelectric ceramic bimorphs. A wave was produced by a displacement in the source transducer due to applied excitation voltage equal to 10 V. A wave transmission created a displacement in the receiver, which in turn resulted in a voltage that could be measured. The frequency of the input signal was variable and decreased from the value f = 10 to f = 3.57 kHz (for lower pressure) or to f = 5.56 kHz (for higher pressure). This frequency range was used in order to reduce the near field effect [54]. According to Camacho-Tauta et al. [60], the undesirable near field effect can be minimized by an appropriate selection of frequency (or period). Properly high frequency of the shear wave increases the ratio between the travel distance (L_{TT}) and the wavelength (λ). Different researchers have given different values of this ratio [61], suggesting keeping it, e.g., between 2.0 and 9.0 [60]. The authors, following recommendations of Leong et al. [62], found it satisfactory to provide L_{TT}/λ ratio >3.0 in order to keep off the near field effect.

Four time domain methods were employed here to compute shear wave velocity (V_S) for all tested specimens, namely: peak-to-peak, zero crossing, first bump and cross-correlation technique. The method peak-to-peak was used twice, the first time in the software during the tests, and again, in the analysis of all the data in the spreadsheet. Additionally, one frequency domain method was applied as well, i.e., cross-power spectrum technique. However, due to the high interference in the signal's beginning, the values of shear wave velocity by first bump method were very inconsistent. Therefore, the authors missed them in the presentation of the results in the next section.

4. Tests Results and Discussion

In Tables 3 and 4, a summary of the V_S values obtained by various techniques of travel time determination is presented. The data combined in Table 3 concern the first three specimens, namely of pure RCA, while those of Table 4 relate to three mixtures of RCA with rubber chips. All the results are resumed here, regardless of whether L_{TT}/λ ratio is greater than 3.0 or not. The wave periods employed in the presented tests, divided into two groups: for specimens No. 1, 4, 6 and for specimens No. 2, 3, 5, arise from the authors' experience and the possibility of clear wave reading. From Tables 3 and 4, it can be noted that the V_S values are not uniform for different periods.

(**a**) (**b**)

Figure 8. Triaxial apparatus device with Bender Elements. (**a**) Triaxial apparatus; (**b**) bender elements, bottom: transmitter, top: receiver.

Table 3. Shear wave velocity (V_S) of pure RCA specimens by four different methods of interpretation and three different mean effective stresses.

Pure RCA No. 1												
p' = 45 kPa	**Period (ms)**		0.10	0.12	0.14	0.16	0.18	0.20	0.22	0.24	0.26	0.28
	Peak-to-peak_1	V_S (ms^{-1})	186.9	186.1	185.1	184.3	182.9	181.8	181.0	179.7	178.0	177.6
	Peak-to-peak_2		187.2	186.4	184.9	183.5	182.2	181.7	180.7	180.0	178.5	177.0
	Zero crossing		272.2	197.4	193.8	193.6	191.0	188.8	187.4	185.8	184.3	182.7
	Cross correlation		181.7	181.7	181.2	181.0	180.8	180.2	179.5	178.2	176.6	174.2
	Frequency domain		184.3	180.7	181.2	180.7	181.2	180.2	181.5	178.5	178.2	173.0
Pure RCA No. 2												
p' = 90 kPa	**Period (ms)**		0.10	0.11	0.12	0.13	0.14	0.15	0.16	0.17	0.18	-
	Peak-to-peak_1	V_S (ms^{-1})	252.6	252.3	251.3	251.5	251.5	250.5	249.9	249.7	249.4	-
	Peak-to-peak_2		253.4	253.1	251.3	251.5	251.8	251.0	250.2	249.4	250.7	-
	Zero crossing		261.8	261.8	260.1	259.5	259.0	257.8	256.7	256.2	255.1	-
	Cross correlation		252.3	253.4	252.9	252.9	252.9	251.8	250.7	248.6	245.0	-
	Frequency domain		258.4	257.8	257.3	258.4	263.6	248.6	265.3	250.2	251.3	-
Pure RCA No. 3												
p' = 180 kPa	**Period (ms)**		0.10	0.11	0.12	0.13	0.14	0.15	0.16	0.17	0.18	-
	Peak-to-peak_1	V_S (ms^{-1})	294.9	294.1	293.8	293.8	293.8	294.1	293.4	293.4	291.3	-
	Peak-to-peak_2		295.6	294.5	293.4	294.5	292.7	294.5	294.1	294.5	292.0	-
	Zero crossing		310.6	308.3	360.1	302.2	299.2	296.3	293.4	291.3	288.6	-
	Cross correlation		296.3	297.0	297.0	297.0	296.3	295.6	292.7	289.3	283.2	-
	Frequency domain		299.9	301.4	299.2	300.7	301.4	302.9	301.4	283.2	283.2	-

Moreover, a comparison of the V_S results obtained by peak-to-peak method, but done twice, shows a big consistency of the values of shear wave velocity. The average difference between the velocities from the technique peak-to-peak_1 and peak-to-peak_2 does not exceed 0.5%, what can be also confirmed in the next presented tables. It follows that it does not matter when the analysis of the signals is performed, during or after the tests.

Table 4. Shear wave velocity (V_S) of mixtures of RCA with rubber chips by four different methods of interpretation and three different mean effective stresses.

RCA with Rubber Chips No. 4												
p' = 45 kPa	**Period (ms)**		0.10	0.12	0.14	0.16	0.18	0.20	0.22	0.24	0.26	0.28
	Peak-to-peak_1	V_S (ms^{-1})	103.3	103.1	102.0	101.4	100.9	100.3	100.0	99.6	99.4	98.6
	Peak-to-peak_2		103.2	103.5	102.3	101.1	102.4	100.5	100.4	99.7	99.5	98.5
	Zero crossing		240.0	251.4	159.2	160.6	112.9	111.5	111.2	109.7	108.8	107.9
	Cross correlation		135.5	93.4	94.2	94.9	95.1	95.3	95.3	95.5	95.4	95.4
	Frequency domain		95.1	101.3	185.5	118.8	137.9	111.2	113.9	129.1	111.5	112.8
RCA with Rubber Chips No. 5												
p' = 90 kPa	**Period (ms)**		0.10	0.11	0.12	0.13	0.14	0.15	0.16	0.17	0.18	-
	Peak-to-peak_1	V_S (ms^{-1})	113.5	112.5	111.8	111.1	110.8	110.1	110.4	110.6	110.6	-
	Peak-to-peak_2		114.1	113.0	112.4	111.5	110.9	109.9	109.8	110.0	110.7	-
	Zero crossing		265.4	184.6	266.0	125.6	124.9	124.3	123.6	122.8	122.8	-
	Cross correlation		370.3	103.2	63.8	104.8	105.0	105.3	105.3	105.3	105.1	-
	Frequency domain		363.8	312.3	128.3	286.3	125.7	129.4	130.6	131.9	132.8	-
RCA with Rubber Chips No. 6												
p' = 180 kPa	**Period (ms)**		0.10	0.12	0.14	0.16	0.18	0.20	0.22	0.24	0.26	0.28
	Peak-to-peak_1	V_S (ms^{-1})	150.2	150.0	149.8	149.1	147.9	147.3	146.5	145.6	144.9	143.7
	Peak-to-peak_2		150.1	149.7	150.8	150.1	148.1	147.5	145.7	145.5	145.5	144.2
	Zero crossing		184.4	204.5	218.4	349.4	561.9	271.8	158.4	156.4	155.7	155.7
	Cross correlation		143.6	142.9	142.5	141.7	141.6	141.2	141.0	140.6	140.3	140.1
	Frequency domain		173.3	147.9	149.1	147.9	144.0	143.2	142.9	143.0	143.2	142.7

In the next order, the statistical analysis of all data from Tables 3 and 4 was executed. Its results are summarized in Tables 5 and 6. The minimum value of V_S in the most cases was received from cross correlation method, whereas the maximum from zero crossing method. The average median value of V_S for specimens tested under p' = 45 kPa is equal to 183.1 m/s, pure RCA, and 43% less, 104.5 m/s, composition of RCA with rubber chips. For specimens tested under p' = 90 kPa, the median value for pure RCA is about 254.3 m/s and more than 50% less, 116.7 m/s, for its composition with rubber chips. A similar difference, namely 47%, is occurred for the average median values of V_S between specimens No 3 and 6 that are respectively 296.9 and 156.7 m/s.

Analyzing other statistical parameters, e.g., dispersion of the results within a method, standard deviation, standard error and variance, the highest values were usually found for zero crossing interpretation method. Regardless of the type of a test material, it can be seen that this technique deviates significantly from others. A large spread of the results is characteristic as well for frequency domain method. It is higher, up to 93%, for composition of RCA with rubber chips than for pure RCA specimens. The smallest spread of the results provides peak-to-peak method, in the region of 1.1 m/s (specimen No. 5) to 4.7 m/s (specimen No. 4). For some specimens (No. 1 and 6) though, a small scatter of the results is obtained by cross correlation method, amounting to 7.5 and 2.8 m/s.

After estimating standard error, it can be noticed that for most of the techniques of travel time identification in BEs testing standard error is minor, except for cross correlation. In general, it does not exceed the value of 1.3 m/s for pure anthropogenic material and 4.4 m/s for its modified version. The above-given data relates to frequency domain method. This means that the chosen interpretation methods are correct. The differences between empirical and theoretical values of V_S hardly exist. The average error in V_S calculation using one of the analyzed method deviates from the theoretical value of V_S by the standard error value (Tables 5 and 6). However, it should be remembered that presented errors do not exactly tell about the scale of the phenomenon. They should be also considered in relation to average value of V_S for each method. Excluding zero crossing method, for pure RCA specimens' standard errors are from 0.2% to 0.4% of the average value of V_S, and for RCA with rubber

chips from 0.4% to 3.3%. This actually confirms the small values of errors as well as the accuracy of the interpretation methods chosen.

Table 5. Result of statistical analysis of pure RCA specimens from different methods of travel time identification in bender element testing.

Pure RCA No. 1											
	Method		Min value	Median value	Max value	Dispersion	Std. deviation	Std. error	Variance	Average value	Uncertainty
p' = 45 kPa	Peak-to-peak_1	V_S (ms^{-1})	177.6	182.4	186.9	9.3	3.3	0.8	10.8	182.3	1.8%
	Peak-to-peak_2		177.0	182.0	187.2	10.2	3.3	0.8	11.1	182.2	1.8%
	Zero crossing		182.7	189.9	272.2	89.5	26.6	2.3	706.5	197.7	13.4%
	Cross correlation		174.2	180.5	181.7	7.5	2.5	0.7	6.1	179.5	1.4%
	Frequency domain		173.0	180.7	184.3	11.3	3.0	0.8	8.8	178.0	1.6%
Pure RCA No. 2											
	Method		Min value	Median value	Max value	Dispersion	Std. deviation	Std. error	Variance	Average value	Uncertainty
P' = 90 kPa	Peak-to-peak_1	V_S (ms^{-1})	249.4	251.3	252.6	3.2	1.1	0.8	1.3	251.0	0.5%
	Peak-to-peak_2		249.4	251.3	253.4	4.0	1.3	0.5	1.6	251.4	0.5%
	Zero crossing		255.1	259.0	261.8	6.7	2.4	0.7	5.7	258.7	0.9%
	Cross correlation		245.0	252.3	253.4	8.4	2.8	0.7	7.6	251.2	1.1%
	Frequency domain		248.6	257.8	265.3	16.7	5.8	1.1	33.2	256.8	2.2%
Pure RCA No. 3											
	Method		Min value	Median value	Max value	Dispersion	Std. deviation	Std. error	Variance	Average value	Uncertainty
p' = 180 kPa	Peak-to-peak_1	V_S (ms^{-1})	291.3	293.8	294.9	3.6	1.0	0.4	0.6	293.6	0.3%
	Peak-to-peak_2		292.0	294.5	295.6	3.6	1.1	0.5	1.2	294.0	0.3%
	Zero crossing		288.6	299.2	360.1	71.5	21.8	2.1	472.9	305.6	7.1%
	Cross correlation		283.2	296.3	297.0	13.8	4.7	1.0	22.5	293.8	1.6%
	Frequency domain		283.2	300.7	302.9	19.7	7.9	1.3	62.6	297.0	2.7%

Table 6. Result of statistical analysis of mixtures of RCA with rubber chips from different methods of travel time identification in bender element testing.

RCA with Rubber Chips No. 4											
	Method		Min value	Median value	Max value	Dispersion	Std. deviation	Std. error	Variance	Average value	Uncertainty
p' = 45 kPa	Peak-to-peak_1	V_S (ms^{-1})	98.6	100.6	103.3	4.7	1.6	0.6	2.5	100.9	1.6%
	Peak-to-peak_2		98.5	100.8	103.5	5,0	1.7	0.6	2.8	101.1	1.7%
	Zero crossing		107.9	112.2	251.4	143.5	55.7	3.3	3107.2	147.3	37.8%
	Cross correlation		93.4	95.3	135.5	42.1	12.8	1.6	164.9	99.0	13.0%
	Frequency domain		95.1	113.4	185.5	90.4	25.5	2.3	652.7	121.7	21.0%
RCA with Rubber Chips No. 5											
	Method		Min value	Median value	Max value	Dispersion	Std. deviation	Std. error	Variance	Average value	Uncertainty
p' = 90 kPa	Peak-to-peak_1	V_S (ms^{-1})	110.1	110.8	113.5	3.4	1.1	0.5	1.3	111.3	1.0%
	Peak-to-peak_2		109.8	110.9	114.1	4.3	1.5	0.6	2.3	111.4	1.4%
	Zero crossing		122.8	124.9	266.0	143.2	61.9	3.5	3836.0	162.2	38.2%
	Cross correlation		63.8	105.1	370.3	306.5	91.2	4.3	8319.3	129.8	70.3%
	Frequency domain		125.7	131.9	363.8	238.1	97.5	4.4	9514.9	193.5	50.4%
RCA with Rubber Chips No. 6											
	Method		Min value	Median value	Max value	Dispersion	Std. deviation	Std. error	Variance	Average value	Uncertainty
p' = 180 kPa	Peak-to-peak_1	V_S (ms^{-1})	143.7	147.3	150.0	6.3	2.2	0.7	4.9	147.2	1.5%
	Peak-to-Peak_2		144.2	147.5	150.8	6.6	2.4	0.7	5.6	147.5	1.6%
	Zero crossing		155.7	204.5	561.9	406.2	134.9	5.2	18200.9	248.0	54.4%
	Cross correlation		140.1	141.2	142.9	2.8	1.0	0.4	0.9	141.3	0.7%
	Frequency domain		142.7	143.2	149.1	6.4	2.6	0.7	6.8	144.9	1.8%

An analysis of uncertainty was also required, in order to approve the precision and credibility of this study. Relative uncertainty in the range of 0.1% to 10% is typical for laboratory experiments. Based on data summarized in Tables 5 and 6, it can be seen, that uncertainty of the results is at the level of 1–2% (specimens No. 1–3) and of 1.4%–30% (specimens No. 4–6), where the highest value was obtained for specimen No. 5. It is clear, that the time domain methods allow for very accurate measurement of V_S, the lowest uncertainty of the results.

In Table 7, selected statistical parameters, i.e., dispersion, standard deviation and standard error, from all four methods together for each specimen are summarized. Pure RCA specimens are characterized by lower values of these parameters (from 50% to 90%), especially specimen No. 2, tested at p' = 90 kPa, than three mixtures of RCA with rubber chips. In the case of composite, No. 5, tested as well at p' = 90 kPa, the values of dispersion, standard deviation and error are the highest. Judging, for example, these two specimens, No. 2 and 5, investigated under the same mean effective stress, the difference between statistical parameters is up to 90%.

Table 7. Comparison of selected parameters of statistical analysis between different methods of travel time identification in bender element testing.

Specimen	No. 1	No. 2	No. 3	No. 4	No. 5	No. 6
			Average			
Dispersion	18.44	10.0	16.8	60.5	108.2	100.1
Std. deviation	7.7	4.2	7.2	25.6	46.9	43.3
Std. error	1.1	0.9	1.1	2.1	2.7	2.5

In Figures 9–11, a graphic variation of the V_S values with a predetermined wave's propagation period at different specified stress level is shown. Besides, it is also a graphic comparison between the time domain and frequency domain techniques of BEs results interpretation. It is important, that for these figures, only the data when the ratio L_{TT}/λ was greater than 3.0 were selected. Plain RCA specimens showed higher sensitivity to the near field effect, since in their case, it was rather difficult to keep the ratio L_{TT}/λ at the appropriate level.

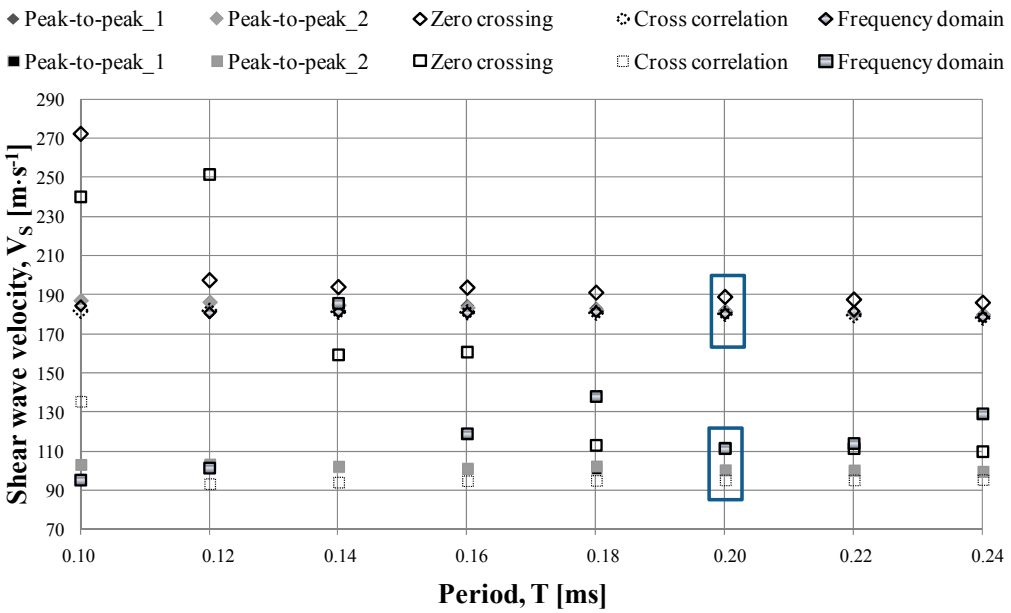

Figure 9. Variation of V_S with period for p' = 45 kPa. Diamond symbols: pure RCA specimens; rectangle symbols: compositions of RCA with rubber chips.

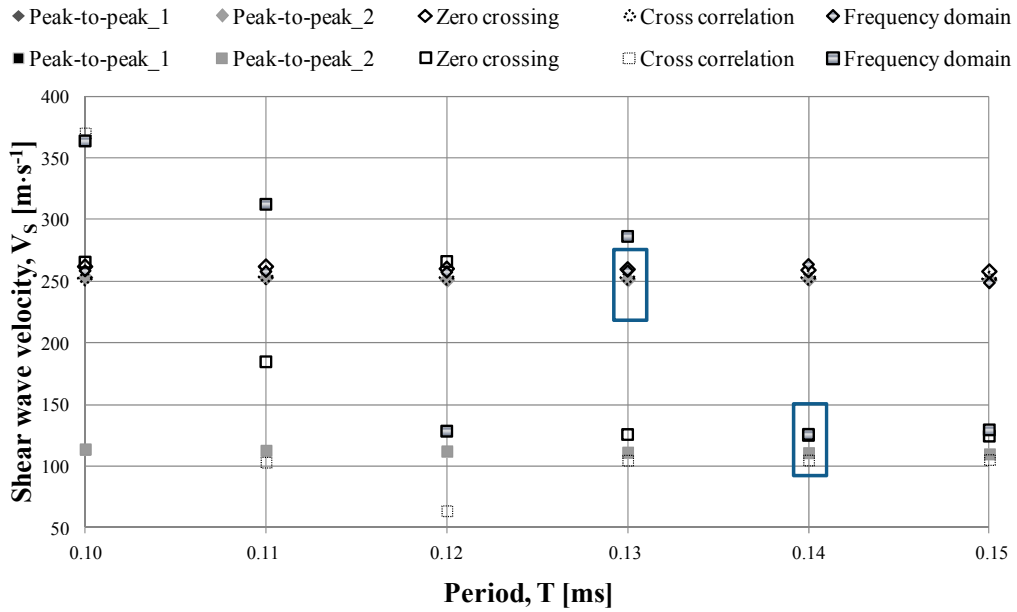

Figure 10. Variation of V_S with period for p' = 90 kPa. Diamond symbols: pure RCA specimens; rectangle symbols: compositions of RCA with rubber chips.

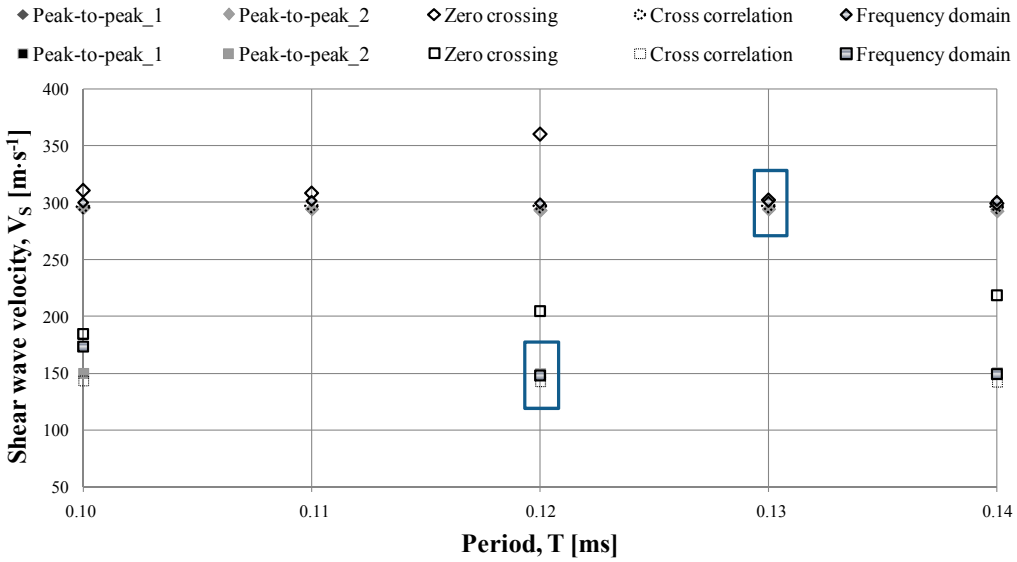

Figure 11. Variation of V_S with period for p' = 180 kPa. Diamond symbols: pure RCA specimens; rectangle symbols: compositions of RCA with rubber chips.

Based on these figures, and in particular, Figures 9 and 11, the conclusion regarding zero crossing method from the statistical analysis is confirmed. Most differs this method from the others. Therefore, in the analysis of the results for p' = 45 kPa and p' = 180 kPa it was removed, completely or partially.

In all the figures, the values of shear wave velocity for compositions of RCA with rubber chips are distinctly lower and less consistent in comparison to pure RCA specimens. A great dispersion of these results is strongly remarkable. The exact values of the spread of the results, comparing two tested materials, are given in Table 7.

Subsequently, for further discussion, from each figure (Figures 9–11) certain wave's periods were chosen, for which wave velocities were nearly identical at given mean effective stress. The selected periods differed slightly, depending on whether pure RCA or mixtures of RCA with rubber chips were analyzed, and what was the level of p' Then, from these wave periods finally one (marked by

rectangle in Figures 9–11) was chosen, for which the difference between the V_S values from different methods was the lowest, from 1% up to maximum 16%. There are the following periods: T = 0.20 ms for p' = 45 kPa, specimens No. 1 and 4, T = 0.13 and 0.14 ms for p' = 90 kPa, specimens No. 2 and 5, T = 0.13 and 0.12 ms for p' = 180 kPa, specimens No. 3 and 6.

Based on the selected periods, the characteristic shear wave velocities were eventually received. In Figure 12, the above-mentioned V_S values are shown as a function of mean effective stress, in order to compare with the reference method. The shear wave velocities vary between 180.2 and 302.1 m/s, as well as between 95.3 and 150.0 m/s (Figure 12). In the case of modified concrete recycled aggregate, the test results are again more scattered. This can be explained, e.g., by the properties and behavior of rubber themselves. Rubber chips do not absorb water and behave differently that grain of soil. Hence, they cannot be saturated with water when the specimen is being saturated and can be very mobile during wave's propagation. They can move simply inside the specimen. Two identical measurements are performed, but the conditions inside the specimen tested are already different, because of various arrangements of rubber grains. Therefore, in the case of this modified material, it is difficult to get consistent results.

It is evident that, regardless of the type of a test material, the V_S values increase with the increase in the p' values. As far as pure RCA specimens are concerned, this is an increase of an average of 29% when p' changes from 45 to 90 kPa, and of 14% with an increase in p' from 90 to 180 kPa. At first, V_S changes are greater, than smaller, with higher p'. In the case of modified RCA, the V_S values increase of about 10% and 23%, when mean effective stress increases respectively from 45 to 90 kPa and from 90 to 180 kPa. Here, the trend of V_S changes is reverse, first there are smaller, than greater changes.

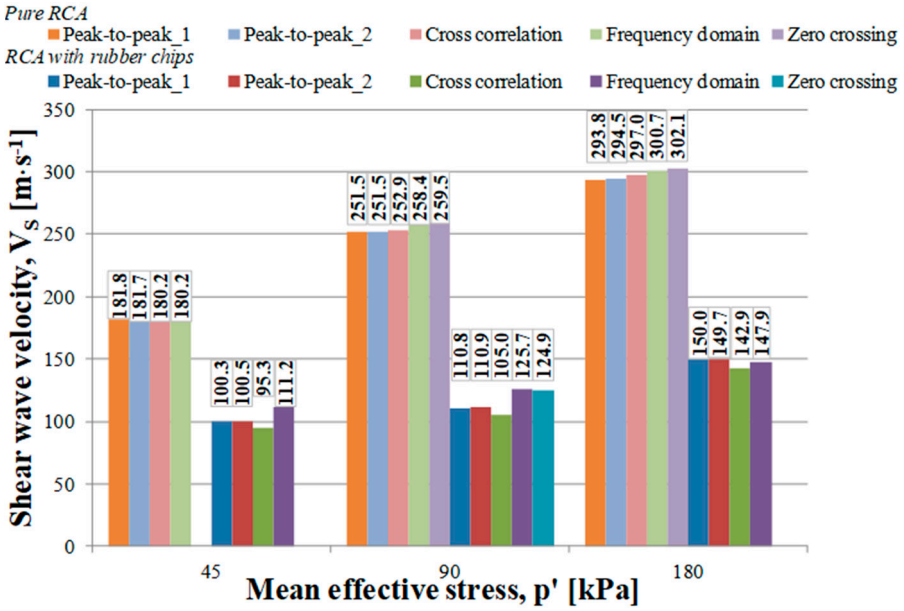

Figure 12. Comparison between selected V_S values of pure RCA specimens and RCA with rubber chips compositions by four/five different methods of interpretation.

According to Figure 12, the highest V_S values can be establish using zero crossing technique, next frequency domain and cross correlation, but only for higher stresses. This finding is not in concordance with the results for p' = 45 kPa, where the highest V_S give peak-to-peak methods. However, the difference between the various methods of BEs results interpretation is at the level of from 1% to the maximum 3%.

As it can be seen in Figure 12, the highest V_S values for RCA with rubber chips at p' = 45 and 90 kPa concerns frequency domain method, whereas at p' = 180 kPa—peak-to-peak method. On the other hand, cross correlation method produces the lowest V_S values, in spite of the stress level. Moreover,

the higher difference between the various methods of BEs results interpretation than for rubber-soil mixtures can be observed, i.e., from 5% to the maximum 16%.

Figures 13–15 represent a comparison between the results for both examined materials: pure RCA and its composition with rubber. In the case of any applied methods of determination of shear wave velocity, the replacement of RCA by rubber chips, for 15%, causes a reduction in the V_S values. It is shown that this decrease in wave velocities is of the order of 20–40%, depending on the p' values. Generally, the same tendency is observed for all the mean effective stresses. With an increase in p', the greater differences in the V_S values for two tested materials are observed. This trend was predictable. According to the literature [35], due to rubber insertion into soil, stiffness of this type of composition decreases, and then the V_S values too. RCA with rubber chips is softer material than pure RCA, because rubber itself is softer than soil. The softer is the system, the lower are the wave velocities and the more diverse.

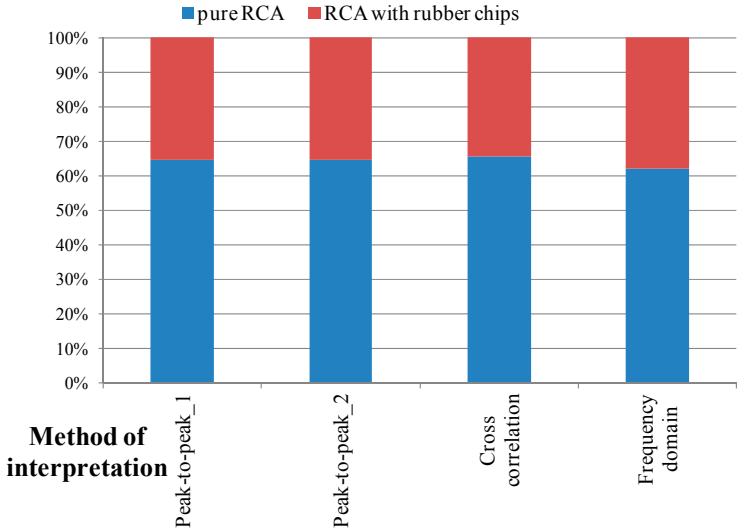

Figure 13. Percentage distribution of V_S values between two different materials: pure RCA and RCA with rubber chips for p' = 45 kPa.

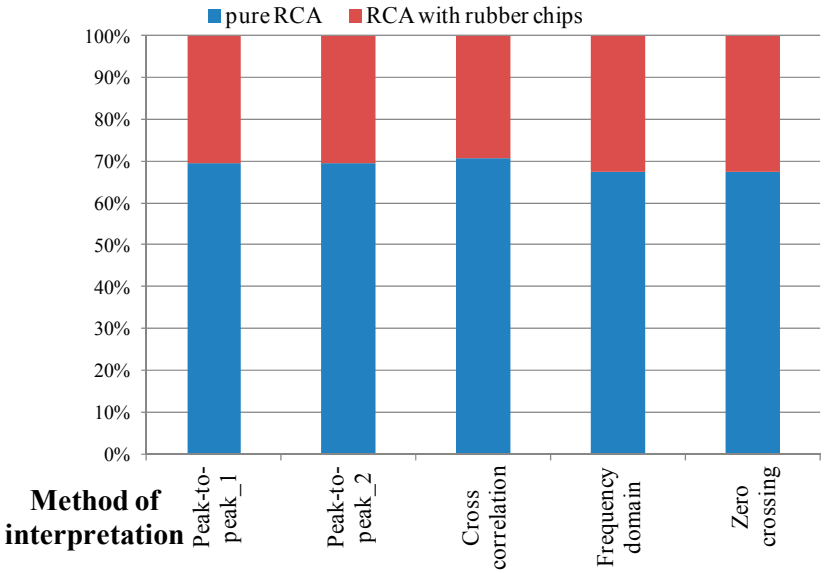

Figure 14. Percentage distribution of V_S values between two different materials: pure RCA and RCA with rubber chips for p' = 90 kPa.

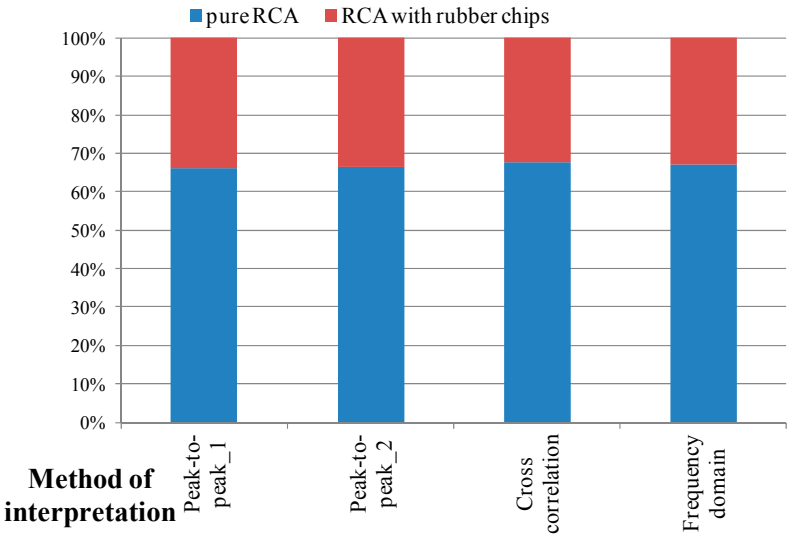

Figure 15. Percentage distribution of V_S values between two different materials: pure RCA and RCA with rubber chips for p' = 180 kPa.

5. Summary and Conclusions

This paper presents the results of bender elements (BEs) tests on anthropogenic soil—Recycled Concrete Aggregate (RCA), and its modified version—a mixture with rubber grains. In this study, dynamic properties of these two artificial materials in terms of shear wave velocity (V_S) are presented.

The main observations from this study are as follows:

1. Shear wave velocity of modified anthropogenic soil is influenced by the rubber content. Concerning the amount of rubber content used, 15% by RCA volume, all three compositions exhibit lower V_S values than pure RCA specimens, up to 40%. This can be explained by insignificant contribution of soft rubber particles on shear wave velocity of mixture solid skeleton. Normal soil (0% rubber) is stiffer, due to greater values of V_S and thus higher shear modulus. The addition of rubber makes the material softer. Another advantage of using rubber grains is less susceptibility to the near field effect. Additionally, regarding the tested mixtures, the results are more scattered, without any consistency. This can be due to the properties and behavior of rubber itself. Rubber grains may be differently arranged in the specimen during the test set on the same specimen.
2. The results of this research present the behavior of mixtures of materials with non-optimized compositions. In order to better examine the effect of rubber inclusion on dynamic properties of modified anthropogenic soil, different combination of soil and rubber chips should be tested. Such research would be helpful in determining the eventual limit in the rubber amount that does not make any significant changes in the dynamic properties of such mixtures.
3. The results of shear wave velocity of pure RCA specimens and RCA-rubber compositions that were obtained by means of peak-to-peak_1 and peak-to-peak_2 techniques are in a good agreement. The average difference between the velocities from both methods does not exceed 0.5%. It is appropriate to make the wave's propagation analysis during BEs test and after it.
4. Application of different interpretation methods of BEs tests in this study suggests rejection of zero crossing method, due to rather overestimated V_S values, up to a maximum of 33% for pure RCA specimens and 76% for RCA-rubber compositions. The minimum value of V_S, in the most analyzed cases, is received from cross correlation method. These values are lower than the average V_S values in the range of 1% to 40%. On the other hand, the higher shear wave velocities are obtained from the frequency domain technique, especially for modified RCA specimens. These values are higher than the average V_S values in the range of 2% to 32%.

5. The time domain methods (e.g., peak-to-peak) provide results that are more consistent. The spread of the results for peak-to-peak method is from 5.5 (pure RCA specimens) to 70 (modified RCA specimens) times lower than for frequency domain, which is considered to be the second method with the greatest spread of the results after zero crossing. This can indicate that for BEs testing in anthropogenic soil the time domain methods are more reliable.
6. The small values of standard error, maximum 1.3 m/s for pure anthropogenic material and 4.4 m/s for its modified version using frequency domain method, may prove the accuracy in the choice of methods for analyzing of the test results. A similar conclusion can be drawn by analyzing how much of the average value of V_S represents standard error. For pure RCA specimens, standard errors are from 0.2% to 0.4% of the average value of V_S, and for RCA with rubber chips, from 0.4% to 3.3%.
7. By means of uncertainty analysis, the precision and reliability of performed laboratory tests can be confirmed. In the most cases, relative uncertainty is in the range of 0.1% to 10%, what is most correct. The lowest uncertainty of the results is received for the time domain methods. It is from 4.4 to 70 times less than the greatest uncertainty.
8. The results of this investigation should be expanded with more samples to give a complete statistical solidity of the indicated behavior.
9. Given the variability in the results, after Jovičić et al. [63], the authors strictly recommend the use of various methods of travel time identification in bender element testing.
10. It would seem a good solution to imply a comparison between the results from BEs tests and, e.g., resonant column (RC) tests. However, in the light of the latest research and reports on natural soils, the results from the most known and modern techniques, like bender elements (BEs) and resonant column (RC) should not be compared. This is because, for example, the excitation frequency and the range of expected strains are different. According to the authors' opinion, nevertheless it would be advisable to do more studies with different experimental techniques. They allow correlating and validating the behavioral results indicated in this research.

Acknowledgments: This research was possible thanks to the equipment co-financed by the European Union from the European Regional Development Fund; Operational Program Infrastructure and Environment 2007–2013, Action 13.1.

Author Contributions: Katarzyna Gabryś and Wojciech Sas conceived and designed the experiments; Emil Soból and Andrzej Głuchowski performed the experiments; Katarzyna Gabryś analyzed the data and wrote the paper; Wojciech Sas edited and audited the content.

Conflicts of Interest: The authors declare no conflict of interest.

References

1. Xu, D.S.; Borana, L.; Yin, J.H. Measurement of small strain behavior of a local soil by fiber Bragg grating-based local displacement transducers. *Acta Geotech.* **2014**, *9*, 935–943. [CrossRef]
2. Kulkarni, M.P.; Patel, A.; Singh, D.N. Application of shear wave velocity for characterizing clays from coastal regions. *KSCE J. Civ. Eng.* **2010**, *14*, 307–321. [CrossRef]
3. Karray, M.; Hussien, M.N. Shear wave velocity as function of cone penetration resistance and grain size for Holocene-age uncemented soils: A new perspective. *Acta Geotech.* **2017**. [CrossRef]
4. El-Sekelly, W.; Tessari, A.; Abdoun, T. Shear Wave Velocity Measurement in the Centrifuge Using Bender Elements. *Geotech. Test. J.* **2014**, *37*, 689–704. [CrossRef]
5. Tun, M.; Ayday, C. Investigation of correlations between shear wave velocities and CPT data: A case study at Eskisehir in Turkey. *Bull. Eng. Geol. Environ.* **2016**. [CrossRef]
6. Shen, M.; Chen, Q.; Zhang, J.; Gong, W.; Juang, C.H. Predicting liquefaction probability based on shear wave velocity: An update. *Bull. Eng. Geol. Environ.* **2016**, *75*, 1199–1214. [CrossRef]

7. Andrus, R.D.; Stokoe, K.H. Liquefaction Resistance Based on Shear Wave Velocity. In Proceedings of the NCEER Workshop on Evaluation of Liquefaction Resistance of Soils, Salt Lake City, Utah, USA, 5–6 January 1996; NCEER-97-0022; National Centre for Earthquake Engineering Research: Buffalo, NY, USA, 1997; pp. 89–128.
8. Zekkos, D.; Sahadewa, A.; Woods, R.D.; Stokoe, K.H. Development of Model for Shear Wave Velocity of Municipal Solid Waste. *J. Geotech. Geoenviron. Eng.* **2014**, *140*. [CrossRef]
9. Lee, M.-J.; Choo, H.; Kim, J.; Lee, W. Effect of artificial cementation on cone tip resistance and small strain shear modulus of sand. *Bull. Eng. Geol. Environ.* **2011**, *70*, 193–201. [CrossRef]
10. Sas, W.; Gabryś, K.; Szymański, A. Experimental studies of dynamic properties of Quaternary clayey soils. *Soil Dyn. Earthq. Eng.* **2017**, *95*, 29–39. [CrossRef]
11. Cha, M.; Santamarina, J.C.; Kim, H.-S. Small-Strain Stiffness, Shear-Wave Velocity and Soil Compressibility. *J. Geotech. Geoenviron. Eng.* **2014**. [CrossRef]
12. Wągrowska, M.; Woźniak, C. On the modeling of dynamic problems for viscoelastic composites. *Int. J. Eng. Sci.* **1996**, *34*, 923–932. [CrossRef]
13. Rahman, M.A.; Imteaz, M.; Arulrajah, A.; Disfani, M.M. Suitability of recycled construction and demolition aggregates as alternative backfilling materials. *J. Clean. Prod.* **2014**, *66*, 75–84. [CrossRef]
14. Witkowski, H. Sustainability of self-compacting concrete. *Archit. Civ. Eng. Environ. ACEE J.* **2015**, *8*, 83–88.
15. Mendivil-Escalante, J.M.; Gómez-Soberón, J.M.; Almaral-Sánchez, J.L.; Cabrera-Covarrubias, F.G. Metamorphosis in the Porosity of Recycled Concretes through the Use of a Recycled Polyethylene Terephthalate (PET) Additive. Correlations between the Porous Network and Concrete Properties. *Materials* **2017**, *10*, 176. [CrossRef]
16. Sas, W.; Głuchowski, A.; Szymański, A. The geotechnical properties of recycled concrete aggregate with addition of rubber chips during cyclic loading. In Proceedings of the 5th International Conference on Géotechnique, Construction Materials and Environment—GEOMATE 2015, Osaka, Japan, 16–18 November 2015.
17. Thomas, B.S.; Gupta, R.C.; Panicker, V.J. Recycling of waste tire rubber as aggregate in concrete: Durability-related performance. *J. Clean. Prod.* **2016**, *112*, 504–513. [CrossRef]
18. Liu, H.; Wang, X.; Jiao, Y.; Sha, T. Experimental Investigation of the Mechanical and Durability Properties of Crumb Rubber Concrete. *Materials* **2016**, *9*, 172. [CrossRef]
19. Takano, D.; Chevalier, B.J.; Otani, J. Experimental and numerical simulation of shear behavior on sand and tire chips. In Proceedings of the 14th International Conference of International Association for Computer Methods and Recent Advances in Geomechanics (IACMAG 2014), Kyoto, Japan, 22–25 September 2014; Taylor & Francis Group: London, UK, 2015; pp. 1545–1550.
20. Edil, T.B. A Review of Environmental Impacts and Environmental Applications of Shredded Scrap Tires. In *Scrap Tire Derived Geomaterials—Opportunities and Challenges*; Hazarika, H., Yasuhara, K., Eds.; IT-TDGM 2007; Taylor & Francis Group: London, UK, 2008; pp. 3–18.
21. Ehsani, M.; Shariatmadari, N.; Mirhosseini, S.M. Shear modulus and damping ratio of sand-granulated rubber mixtures. *J. Cent. South Univ.* **2015**, *22*, 3159–3197. [CrossRef]
22. Anbazhagan, P.; Manohar, D.R. Energy absorption capacity and shear strength characteristics of waste tire crumbs and sand mixtures. *Int. J. Geotech. Earthq. Eng.* **2015**, *6*, 30–51. [CrossRef]
23. Padmini, A.K.; Ramamurthy, K.; Mathews, M.S. Influence of parent concrete on the properties of recycled aggregate concrete. *Construct. Build. Mater.* **2009**, *23*, 829–836. [CrossRef]
24. Soból, E.; Sas, W.; Szymański, A. Scale Effect in Direct Shear Tests on Recycled Concrete Aggregate. *Stud. Geotech. Mech.* **2015**, *37*, 45–49. [CrossRef]
25. Arulrajah, A.; Disfani, M.M.; Horpibulsuk, S.; Suksiripattanapong, C.; Prongmanee, N. Physical properties and shear strength responses of recycled construction and demolition materials in unbound pavement base/subbase applications. *Construct. Build. Mater.* **2014**, *58*, 245–257. [CrossRef]
26. Melbouci, B. Compaction and shearing behaviour study of recycled aggregates. *Construct. Build. Mater.* **2009**, *23*, 2723–2730. [CrossRef]
27. Sas, W.; Głuchowski, A.; Szymański, A. Behavior of Recycled Concrete Aggregate Improved with Lime Addition During Cyclic Loading. *Int. J. GEOMATE* **2016**, *10*, 1662–1669. [CrossRef]

28. Aurstad, J.; Aksnes, J.; Dahlhaug, J.E.; Berntsen, G.; Uthus, N. Unbound crushed concrete in high volume roads—A field and laboratory study. In Proceedings of the 5th International Conference on Research and Practical Applications Using Wastes and Secondary Materials in Pavement Engineering, Liverpool, UK, 22–23 February 2006.
29. Liang, C.; Liu, T.; Xiao, J.; Zou, D.; Yang, Q. Effect of Stress Amplitude on the Damping of Recycled Aggregate Concrete. *Materials* **2015**, *8*, 5298–5312. [CrossRef]
30. Sas, W.; Głuchowski, A.; Gabryś, K.; Soból, E.; Szymański, A. Deformation Behavior of Recycled Concrete Aggregate during Cyclic and Dynamic Loading Laboratory Tests. *Materials* **2016**, *9*, 780. [CrossRef]
31. Srinivas, A.; Prasad, D.S.V.; Anjan Kumar, M.; Prasada Raju, G.V.R. Utilization of waste materials in the construction of roads. *Int. J. Eng. Res. Dev.* **2015**, *11*, 55–62.
32. Ghatge, S.H.; Rakaraddi, P.G. Soil stabilization using waste shredded rubber tire chips. *J. Mech. Civ. Eng.* **2014**, *11*, 20–27.
33. Feng, Z.Y.; Sutter, K.G. Dynamic Properties of Granulated Rubber/Sand Mixtures. *Geotech. Test. J.* **2000**, *23*, 338–344. [CrossRef]
34. Mashiri, M.S.; Vinod, J.S.; Sheikh, M.N. Liquefaction Potential and Dynamic Properties of Sand-Tyre Chip (STCh) Mixtures. *Geotech. Test. J.* **2016**, *39*, 69–79. [CrossRef]
35. Senetakis, K.; Anastasiadis, A.; Pitilakis, K. Dynamic Properties of Dry Sand Rubber (SRM) and Gravel/Rubber (GRM) Mixtures in a Wide Range of Shearing Strain Amplitudes. *Soil Dyn. Earthq. Eng.* **2012**, *33*, 38–53. [CrossRef]
36. Turer, A.; Özden, B. Seismic Base Isolation Using Low-Cost Strap Tire Pads (STP). *Mater. Struct.* **2008**, *41*, 891–908. [CrossRef]
37. Kaneko, K.; Orense, R.P.; Hyodo, M.; Yoshimoto, N. Seismic Response Characteristics of Saturated Sand Deposits Mixed with Tire Chips. *J. Geotech. Geoenviron. Eng.* **2013**, *139*, 633–643. [CrossRef]
38. Tsang, H.H.; Lo, S.H.; Xu, X.; Sheikh, M.N. Seismic Isolation for Low-to-Medium-Rise Buildings Using Granulated Rubber-Soil Mixtures: Numerical Study. *Earthq. Eng. Struct. Dyn.* **2012**, *41*, 2009–2024. [CrossRef]
39. Anbazhagan, P.; Manohar, D.R. Small- to Large-Strain Shear Modulus and Damping Ratio of Sand-Tire Crumb Mixtures. In *Geo-Chicago 2016: Sustainable Materials and Resource Conservation*; American Society of Civil Engineers: Chicago, IL, USA, 2016; pp. 305–315.
40. Polish Committee for Standardization. *Tests for Geometrical Properties of Aggregates. Classification Test the Constituents of Coarse Recycled Aggregate*; PN-EN 933-11:2009; BSI: Warsaw, Poland, 2009.
41. WT-4. Unbound Mixtures for National Roads. Available online: http://www.gddkia.gov.pl/userfiles/articles/d/Dokumenty_techniczne/WT4.pdf (accessed on 4 January 2017). (In Polish)
42. Cabrera-Covarrubias, F.G.; Gómez-Soberón, J.M.; Almaral-Sánchez, J.L.; Arredondo-Rea, S.P.; Gómez-Soberón, M.C.; Corral-Higuera, R. An Experimental Study of Mortars with Recycled Ceramic Aggregates: Deduction and Prediction of the Stress-Strain. *Materials* **2016**, *9*, 1029. [CrossRef]
43. European Committee for Standardization. *Geotechnical Design—Part 2: Ground Investigation and Testing*; EN 1997-2:2007; CEN: Brussels, Belgium, 2007.
44. Polish Committee for Standardization. *Geotechnical Investigation and Testing—Identification and Classification of Soil—Part 2: Principles for a Classification*; PN-EN 14688-2:2006; BSI: Warsaw, Poland, 2006.
45. Camacho-Tauta, J.F.; Cascante, G.; Viana da Fonseca, A.; Santos, J.A. Time and frequency domain evaluation of bender element systems. *Géotechnique* **2015**, *65*, 548–562. [CrossRef]
46. Shirley, D.J.; Hampton, L.D. Shear-wave measurement in laboratory sediments. *J. Acoust. Soc. Am.* **1978**, *63*, 607–613. [CrossRef]
47. Kim, T.; Han, J.; Cho, W. Nonlinear stress-strain response of soft Chicago glacial clays. *KSCE J. Civ. Eng.* **2015**, *19*, 1139–1149. [CrossRef]
48. Airey, D.; Mohsin, A.K.M. Evaluation of Shear Wave Velocity from Bender Elements Using Cross-Correlation. *Geotech. Test. J.* **2013**, *36*, 506–514. [CrossRef]
49. Sanchez-Salinero, I.; Roesset, J.M.; Stokoe, K.H.I. *Analytical Studies of Body Wave Propagation and Attenuation*; Report GR 86-15; University of Texas: Austin, TX, USA, 1986.
50. Brignoli, E.G.; Gotti, M.; Stokoe, K.H.I. Measurement of shear waves in laboratory specimens by means of piezoelectric transducers. *Geotech. Test. J.* **1996**, *19*, 384–397. [CrossRef]
51. Arulnathan, R.; Boulanger, R.W.; Reimer, M.F. Analysis of Bender Element Tests. *Geotech. Test. J.* **1998**, *21*, 120–131. [CrossRef]

52. Arroyo, M.; Muir Wood, D.; Greening, P.D.; Medina, L.; Rio, J. Effects of Sample Size on Bender-based Axial G0 Measurements. *Géotechnique* **2006**, *56*, 39–52. [CrossRef]
53. Lee, J.S.; Santamarina, J.C. Bender Elements: Performance and Signal Interpretation. *J. Geotech. Geoenviron. Eng.* **2005**, *131*, 1063–1070. [CrossRef]
54. Sas, W.; Gabryś, K.; Soból, E.; Szymański, A. Dynamic Characterization of Cohesive Material Based on Wave Velocity Measurements. *Appl. Sci.* **2016**, *6*, 49. [CrossRef]
55. Franco, E.E.; Mesa, J.M.; Buiochi, F. Measurement of elastic properties of materials by the ultrasonic through transmission technique. *Rev. Ing. Dyna* **2011**, *78*, 59–64.
56. Viggiani, G.; Atkinson, J.H. Interpretation of bender element tests. *Géotechnique* **1995**, *45*, 149–154. [CrossRef]
57. Greening, P.D.; Nash, D.F.T. Frequency Domain Determination of G0 Using Bender Elements. *Geotech. Test. J.* **2004**, *27*, 1–7. [CrossRef]
58. GDS. Available online: www.gdsinstruments.com (accessed on 4 January 2017).
59. Chan, C.M. Bender Element Test in Soil Specimens: Identifying the Shear Wave Arrival Time. *Electron. J. Geotech. Eng.* **2010**, *15*, 1263–1276.
60. Camacho-Tauta, J.F.; Jiménez Álvarez, J.D.; Reyes-Ortiz, O.S. A procedure to calibrate and perform the bender element test. *Rev. Ing. Dyna* **2012**, *79*, 10–18.
61. Chan, C.M. On the interpretation of shear wave velocity form bender element tests. *Acta Tech. Corviniensis Bull. Eng.* **2012**, *5*, 29–34.
62. Leong, E.-C.; Yeo, S.-H.; Rahardjo, H. Measurements of wave velocities and attenuation using an ultrasonic test system. *Can. Geotech. J.* **2004**, *41*, 844–860. [CrossRef]
63. Jovičić, V.; Coop, M.R.; Simić, M. Objective criteria for determining G_{max} from bender element tests. *Géotechnique* **1996**, *46*, 357–362. [CrossRef]